

Demonstration of helicity conservation during magnetic reconnection using Christmas ribbons

Hans Pfister and Walter Gekelman

Department of Physics, University of California, Los Angeles, California 90024

(Received 27 October 1989; accepted for publication 18 September 1990)

This article shows how a simple Christmas ribbon can be used to demonstrate a relatively complex physical phenomenon: the conservation of helicity during magnetic reconnection. The physical term, helicity, and the process of magnetic reconnection will be introduced and explained in detail. The "helicity meter," a very simple device that will help in the determination of the helicity of certain topological configurations, will also be introduced.

I. INTRODUCTION

More than 99% of our universe as we know it is in the plasma state, the fourth state of matter. In simple terms, a plasma is an ionized gas. Many of the plasmas that are found in space as well as many that are man-made in research laboratories carry electrical currents. In contrast to a current that we might find in an electric wire where only the electrons move through the metallic lattice, a current in a plasma consists of negative electrons moving in one direction and positive ions moving in the opposite direction. Besides, plasma currents are not spatially confined like those in a metallic conductor. Whether the current is in a wire or a plasma, it is always accompanied by its own magnetic field. In a plasma, the sum of all magnetic and electric fields (externally imposed and self-generated fields) determines the details of the current flow.

Some of the more interesting current systems are the so-called "force-free" current configurations. In these the current flows along the magnetic field lines such that the Lorentz force vanishes, i.e., $\mathbf{J} \times \mathbf{B} = 0$ or more generally $\nabla \times \mathbf{B} = \alpha(\mathbf{r})\mathbf{B}(\mathbf{r})$, where \mathbf{J} denotes the current density, \mathbf{B} the magnetic field, and $\alpha(\mathbf{r})$ is a constant that may depend on position.¹⁻³ Force-free current systems are characterized by no net forces on any current filament within them due to the magnetic field generated by all the other current elements. Many current systems observed in space are believed to be force-free. To mention just a few examples: The long persistence of solar prominences is ascribed to the circumstance that the current system is force-free and relaxed to a minimum energy state,⁴⁻⁶ cosmic magnetic fields confining stellar plasmas of low density are believed to be force-free, and electrical currents in the vicinity of magnetic stars seem to be field-aligned.⁷ There are solar corona models that use constant- α fields.⁸⁻¹⁰ The internal field structure of interplanetary magnetic clouds can be represented as a magnetic force-free configuration.¹¹ Furthermore, currents in plasmoids, which are moving blobs of plasma with a magnetic field embedded within them, exhibit this property.¹² Finally, force-free configurations are found in several toroidal plasma configurations.^{13,14} Part of basic plasma physics research is to understand the dynamics of such current systems, the forces that hold them together or cause changes in their internal structure, and the way they relax to a minimum energy state.

In 1958, Woltjer proved, using a variational principle, that force-free fields with constant α represent the state of lowest magnetic energy in a closed system.^{15,16} The only thing that he had to assume to be conserved during the

relaxation process was a physical quantity called helicity. Helicity in simple terms is a measure for the "linkedness," "knottedness," and "twistedness" of magnetic field. It is intuitively compelling that if the magnetic energy is a minimum, the field should produce no motions, and therefore the Lorentz force must vanish. In 1974, Taylor outlined a theory that accounts for the generation of the reversed field in the outer region of a toroidal pinch, and also gave the critical value for which the field reversal of these so-called "reversed field pinches" set in.^{17,18} A remarkable feature of many plasma "pinch" experiments is that after an initial, violently unstable phase, the plasma relaxes into a "quiescent," stable state. Taylor conjectured that the relaxation can only take place under the constraint of conserving the total helicity of the system. The final state must be one where the energy is a minimum subject to this constraint.

Butt *et al.*'s laboratory experiments on a "reversed field pinch" in 1976 supported the Taylor conjecture.¹⁹ They observed a quiescent state similar to the constant- α field. Helicity conservation arguments were also used in the models of solar flares by Norman and Heyvaerts (1983).²⁰ In 1984, Berger placed some geometry-independent limits on helicity dissipation in the presence of resistivity.²¹ In 1985, Königl and Choudhuri used helicity conservation arguments for the treatment of astrophysical jets.²² In his 1987 article, Kadomtsev came to the conclusion that many tokamak experiments show that the plasma tries to retain by itself certain optimal profiles even in the presence of perturbations.²³ He explained this phenomenon of natural profile retention as a result of plasma self-organization via relaxation to the minimum energy state while helicity is conserved. Similarly, Janos (1986) attributes the relaxation of his Spheromak plasma to magnetic reconnection at constant helicity.²⁴

During the reorganization and relaxation process of these current systems, magnetic field lines are allowed to break up and reconnect resulting in simplification of the magnetic topology. At first sight it appears that this process of "magnetic reconnection" cannot possibly conserve magnetic helicity since even in the simplest case of two singly linked magnetic flux tubes, i.e., bundles of magnetic field lines, reconnection takes away the linkage and, thus, the helicity. This, however, is not the case.

In this article we will show how this apparent conflict arises and convince the reader with a very simple demonstration using a ribbon that such reconnection processes indeed conserve magnetic helicity. Before we proceed, let us review the concepts of magnetic reconnection and magnetic helicity.

II. MAGNETIC RECONNECTION

A magnetic field line is a line whose tangent vector points in the direction of the magnetic field at each point along the line. It is an abstract concept, but can be made visible with iron filings scattered on a piece of glass placed on a magnet. A field line can break only if the two free ends that are generated are able to join immediately with the free ends of another simultaneously broken field line. Scientists normally refer to the breaking up of two adjacent, locally antiparallel field lines (cf. field lines 1 and 2 of Fig. 1) and the immediate "reconnection" (parts 1'-2' and 1''-2'' of Fig. 1), as magnetic reconnection. There are many alternate definitions.²⁵

Many examples can be found in nature where magnetic reconnection occurs.^{26,25} There are cases where reconnection is a neverending process as in the magnetotail of the Earth.^{27,28} Far past the Moon's orbit on the antisunward side, the Earth's magnetic field lines look just as depicted in Fig. 1(a). A wealth of satellite data constitutes evidence that magnetic reconnection continually takes place in that region.^{29,30}

We can easily visualize the process of magnetic reconnection by simply using iron filings and either two bar magnets or two horseshoe magnets. Let us take a closer look at the field-line reconnection as two horseshoe magnets approach each other. If the two magnets are far apart, i.e., if the separation between the two magnets is considerably larger than the distance between the two poles of each magnet, then the field lines are almost exclusively concentrated between the north and south pole of each magnet [cf. Fig.

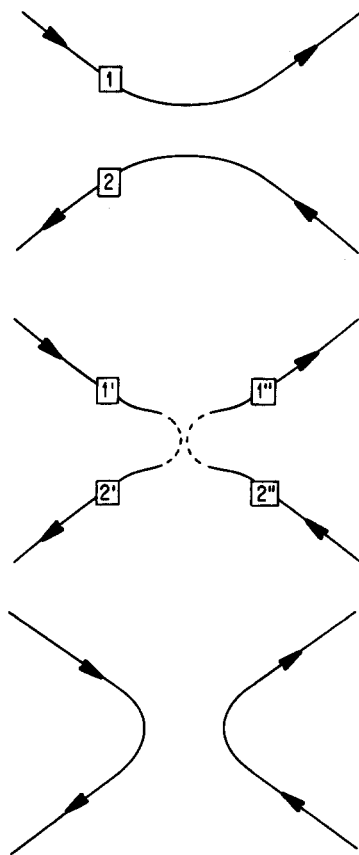


Fig. 1. Reconnection of magnetic field lines.

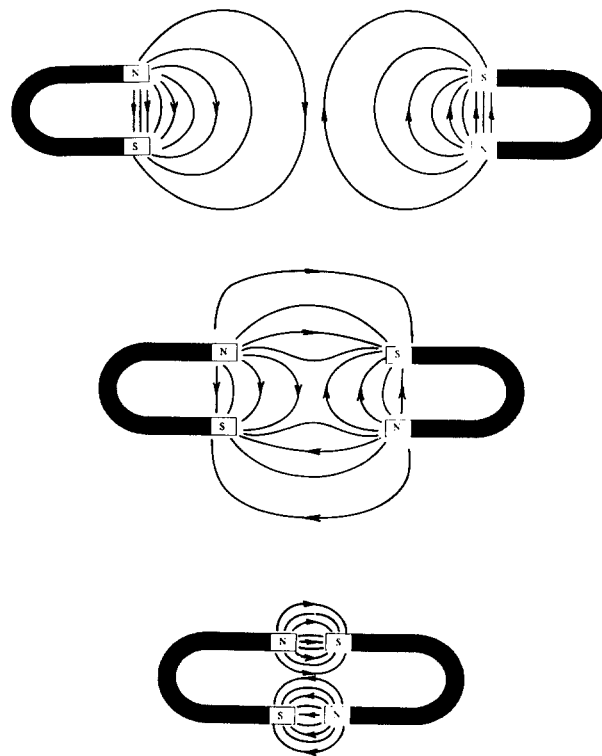


Fig. 2. Reconnection of magnetic field lines between two approaching horseshoe magnets.

2(a)]. In close proximity, however, the field lines outside each magnet mainly connect the north pole of one magnet to the south pole of the other [cf. Fig. 2(c)]. As the magnets are brought together, we witness the transition from one configuration to the other. It is the relative motion of the magnets that is the cause for the reconnection of the magnetic field lines. Notice that the field lines of the intermediate state, depicted in Fig. 2(b), have an "X" shape in the center, the reconnection region. This magnetic "X" configuration is typical for a magnetic reconnection topology. The reconnection occurs actually at the point where the magnitude of the magnetic field evolves through a value of zero. And, of course, the reconnection proceeds in the reverse direction as the two magnets are moved apart again.

III. HELICITY

In simple terms, helicity could be described as a measure of the extent to which a topological configuration is linked, knotted, and twisted. Such a configuration might consist of magnetic field lines, knotted mathematical structures,³¹ DNA molecules, ropes or ribbons, or some yarn that used to be the cat's favorite toy. In the following discussion, we will limit ourselves to magnetic field lines. For the explanation of magnetic helicity, we will be confronted with the physical quantity of magnetic flux and we will also encounter the term "flux tube" or "flux rope."³² Magnetic flux, denoted by the Greek symbol Φ , refers to the amount of magnetic field \mathbf{B} that penetrates a cross-sectional area S and is quantitatively expressed as

$$\Phi = \int \mathbf{B} \cdot d\mathbf{S}, \quad (1)$$

where $d\mathbf{S} = \hat{\mathbf{n}} dS$ denotes a vector normal to the area ele-

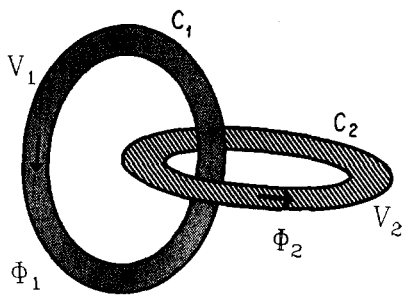


Fig. 3. Two singly linked flux tubes.

ment dS and $\mathbf{B} \cdot d\mathbf{S}$ is the dot product of the magnetic field vector \mathbf{B} with this infinitesimal area vector $d\mathbf{S}$. A flux tube or flux rope represents a bundle of magnetic field lines. Consequently, its surface consists of field lines. Since no field lines leave or enter a flux tube, the flux through any arbitrary cross-sectional area is constant. A flux tube is always a closed topological structure.

First, let us look at the simplest form of linkedness, i.e., two flux tubes of cross-sectional area S_1 and S_2 and of magnetic flux Φ_1 and Φ_2 that are linked as shown in Fig. 3.

Mathematically, magnetic helicity is defined as the integral over the dot product of the magnetic field \mathbf{B} and the magnetic vector potential \mathbf{A} , integrated over the entire volume in which the magnetic field exists.³³

$$H = \int \mathbf{A} \cdot \mathbf{B} dV. \quad (2)$$

The magnetic vector potential and the magnetic field are related via $\mathbf{B} = \nabla \times \mathbf{A}$. If we perform this integration for the example depicted in Fig. 3, we obtain the simple result

$$H = 2\Phi_1 \Phi_2, \quad (3)$$

i.e., twice the product of the individual fluxes of the two flux tubes. (The details are worked out in the Appendix.)

Besides the obvious situations of linked or knotted flux tubes, helicity also may appear disguised in the form of twistedness. Many people automatically associate helicity with linked flux tubes, and some are reluctant to accept the fact that one isolated flux tube that is neither knotted nor interlinked with another flux tube can incorporate helicity! Nevertheless, this does occur when a single flux tube is internally twisted. To confirm this we suggest the reader try taking a piece of electric cord (about 30 cm long) on which both leads can be distinguished, and, while holding one end fixed rotate the other end once in either a clockwise or counterclockwise direction about the axis of the cable such that it has one 360° twist before joining the corresponding ends by using, for example, a soldering iron. Then, separate the two leads from each other by pulling them apart lengthwise and discover that they are linked together! The resulting two *linked* leads demonstrate clearly that the twisted flux tube and two linked flux tubes are close relatives.³⁴ (A detailed inspection of the individual leads reveals that each still has one 360° twist.) We will come back to the details of this relationship in a later section.

IV. MEASURING HELICITY

In the following, for the sake of simplicity but with no loss of generality, let us assume that all flux tubes in a given

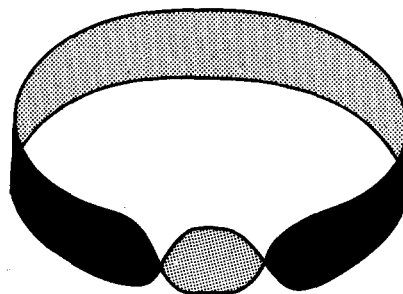


Fig. 4. An O-shaped configuration with one 360° twist.

configuration contain the same flux Φ .³⁵

One way to measure the helicity contained in a twisted flux tube is to imagine a line drawn on the top surface of a flux tube and to count how often a given magnetic field line crosses this imaginary line.³⁶ Instead of pursuing this method, however, we will describe an alternative procedure whereby all twists, links, and knots are converted into "crossings." Let us first consider twists.

The simplest form of "twistedness" appears in an O-shaped configuration that has one full 360° twist in it. Such a configuration, shown in Fig. 4, is easily formed by taking a length of Christmas ribbon twisting it once and joining the ends. We can easily take this configuration and bend it into a figure-8 configuration such that the internal twist disappears. But in doing so we create a "crossing," i.e., the flux tube crosses over itself in the center of the figure-8 as we look down on it. So we have either an O configuration with a full 360° internal twist, or a figure-8 with a crossing and no internal twist, or any situation in between. But surely, no matter how we move, turn, or deform this topological configuration, we cannot change the helicity contained in it.

If we assume that the flux through a cross section of our singly twisted, O-shaped tube is Φ , then the helicity content of this configuration is $H = +\Phi^2$ or $H = -\Phi^2$, depending on the orientation of the twist (clockwise or counterclockwise) as we move along the tube. We call the helicity contained in the O-shaped configuration *one elemental quantum* of helicity, the smallest quantity of helicity that we can imagine.

We would like to point out that a flux tube containing multiple twists can always be turned or deformed such that all twists vanish. But for every twist we successfully get rid of, we create a crossing. Take a Christmas ribbon of approximately $\frac{1}{2}$ -m length and give it, for example, two full twists ($2 \times 360^\circ$) and join the ends. Let us now attempt to eliminate both twists. What we wind up with is an untwisted ribbon with two crossings [cf. Fig. 9(d)]. Of course, the helicity contained in this configuration is either plus or minus $2\Phi^2$. Seemingly, each crossing contributes an amount of plus Φ^2 or minus Φ^2 , respectively, to the total helicity of a configuration depending on the particular type of crossing.

Now let us look at topological configurations containing linkages. The simplest of these is certainly the one we encountered above: two singly linked loops (cf. Fig. 3). We already mentioned that the helicity content of two singly linked, intrinsically untwisted flux tubes having both the same flux Φ , is $H = 2\Phi^2$ or $H = -2\Phi^2$, depending on the linkage. Since we are free to move, turn, and/or deform this linked configuration as we please without changing the he-

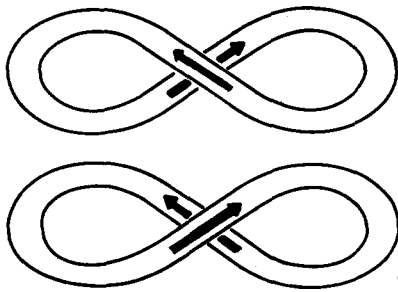


Fig. 5. Figure-8 configurations with one crossing and no internal twist. (a) The helicity contained in this configuration is $H = -\Phi^2$ and (b) the helicity contained in this configuration is $H = +\Phi^2$.

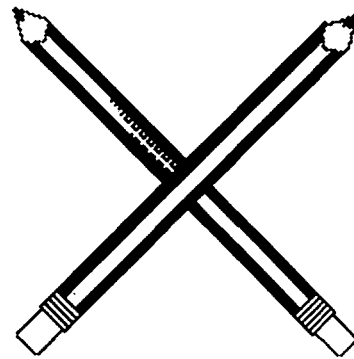


Fig. 6. The "high-tech" pencil helicity meter.

licity content, let us simply lay the two linked rings on a table. We now observe two crossings that locally resemble the crossing of our figure-8. The fact that the figure-8 configuration with one crossing had a helicity content of plus or minus Φ^2 , and the singly linked structure with two apparent crossings has a helicity content of plus or minus $2\Phi^2$, suggests a possibility for "counting" the helicity contained in linked topological configurations.

We have now seen that twists as well as links can be converted to crossings without changing the helicity content of the respective configuration. The same holds true for knots. We can take our knotted configuration, lay it out on a table, and then evaluate the crossings that appear. We immediately realize that there are two different types of crossings. Therefore, let us now take a closer look at these crossings. Figure 5 displays the two basic figure-8 configurations. These are as distinct from each other as a right and a left shoe. If we were to unbend these figure-8 into the singly twisted O configurations, we would find that the one in Fig. 5(a) has a twist in the clockwise direction, and the one in Fig. 5(b) a counterclockwise twist, as we move along the loop. The helicity contained in the flux tube of Fig. 5(a) is $+\Phi^2$, and the helicity contained in the flux tube of Fig. 5(b) is $-\Phi^2$.

If we take a closer look at the crossings in Fig. 3 we recognize that both crossings are of the same type [5(a)-type] and thus the total helicity is $+2\Phi^2$. Each crossing contributes $+\Phi^2$ to the total helicity.

We are now able to give a simple recipe for "counting" the total helicity contained in a topological configuration in which we know the flux of every flux tube involved. First we take a three-dimensional knotted, linked, and twisted configuration that might consist of several flux tubes (remember, for simplicity, we are assuming that all tubes have the same flux³⁵) and lay it on a table to make it quasi-two-dimensional. We then convert all internal twists into crossings as we illustrated above with the doubly twisted Christmas ribbon. Next we must determine the type of each crossing [Fig. 5(a)-type or Fig. 5(b)-type] and then add either $+\Phi^2$ or $-\Phi^2$ to our sum. This counting process is simpler still with our "high-tech" pencil helicity meter that consists of two pencils that are held together by a rubber band as shown in Fig. 6.³⁷ The application of our pencil helicity meter is straightforward: Align it with a crossing and always register a "+1" if the crossing matches the crossing of the pencils, and a "-1" if one of the B-field directions is antiparallel to the directions in which the pencils point. Multiplication of the resulting number by Φ^2 gives the total helicity content of the configuration.

The reader might want to verify that the total helicity of the configuration depicted in Fig. 7 consisting of a "trefoil knot" linked with a simple flux tube is $5\Phi^2$.

Following this procedure of determining the helicity of a topological configuration the reader might get the impression that helicity is something that can be localized at a tube crossing. But these crossings do not have to be at any particular location. They can be moved around as much as the topology allows.

Mathematically, one obtains the total helicity by integrating Eq. (2) over the entire volume of all flux tubes. And, of course, in general, the magnetic field is not as nicely confined to tubes as we assume here.

V. CONNECTION BETWEEN TWISTEDNESS AND LINKEDNESS

We are now able to take a detailed look at the connection between twistedness and linkedness. We will illustrate this with a suitably twisted strip of paper or Christmas ribbon. For this demonstration, we conveniently reuse the ribbon that contains one 360° twist (cf. Fig. 4) which we converted into a figure-8 configuration earlier. The helicity content of this singly twisted flux tube is Φ^2 if we assume a flux of Φ .

In order to demonstrate now the connection between twistedness and linkedness, we take our singly twisted and joined ribbon and cut it lengthwise with a pair of scissors. We obtain two singly linked ribbons, one containing a fraction $f\Phi$ of the flux and the other containing the remaining flux $(1-f)\Phi$, that are still singly twisted. The quantitative distribution of helicity that is contained in links and twists is summarized in Table I. We discover that the helicity content is the same before and after the cutting.

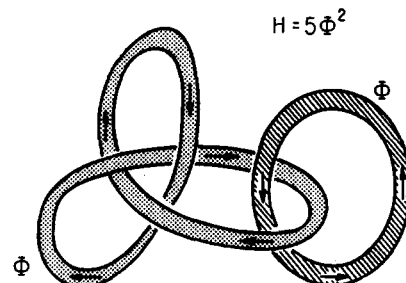


Fig. 7. A trefoil knot singly linked with a single loop.

Table I. Quantitative distribution of helicity that is contained in links and twists.

Before cutting	After cutting		
One full twist of a flux tube with flux Φ	Contribution	of	linkage:
	$2(f\Phi)((1-f)\Phi)$		
	Twist of number 1: $+(f\Phi)^2$		
	Twist of number 2: $++((1-f)\Phi)^2$		
Helicity content: $H = \Phi^2$	total helicity: $H = \Phi^2$		

VI. RECONNECTION AND CONSERVATION OF HELICITY

Having now reviewed the concepts of reconnection and magnetic helicity, and having acquired a tool to measure the total helicity content of a topological configuration, we can look at the relation between reconnection and helicity. There is a common misconception that reconnection cannot possibly conserve helicity. If we imagine a single magnetic field line singly linked with another field line, then, indeed, after reconnecting the two linked loops to a single loop, helicity vanishes as displayed in Fig. 8.

But the picture of a single magnetic field line interlinked with another single field line is an erroneous oversimplification of the *physical* problem. In reality, the smallest "thing" one can have is a flux tube of a finite, albeit small, cross section. Performing the reconnection of two singly linked flux tubes, we end up with no more linkage, but, the reconnected flux tube inevitably appears with an intrinsic twist. We have shown earlier that twistedness is topologically identical to linkedness and, indeed, we now show that the amount of helicity that is contained in this twisted flux tube exactly equals the amount of helicity that was contained in the configuration before the reconnection. We illustrate this circumstance by reconnecting two singly linked loops of untwisted ribbons (corresponding to those displayed in Fig. 3).

For the following demonstration we recommend the use of a Christmas ribbon that is about 1 cm wide or strips of paper cut to this width and joined to form a loop. A 1-m section and a 1/2-m section of untwisted ribbon are linked as shown in Fig. 9(a) and the open ends are joined together.

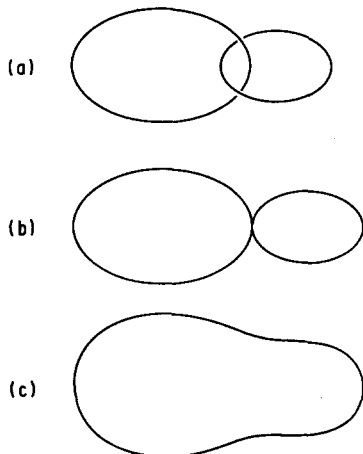


Fig. 8. Erroneous picture of flux tube reconnection.

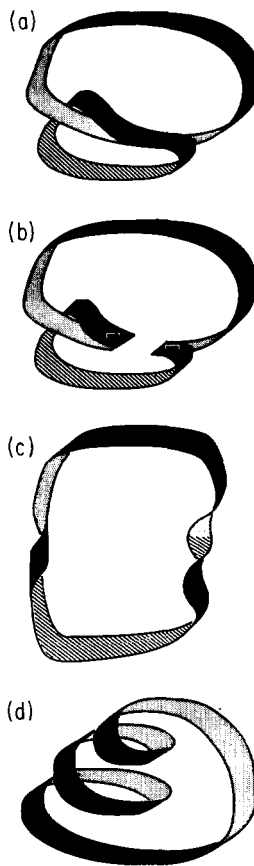


Fig. 9. Reconnection of two singly linked Christmas ribbons.

The reader might want to draw B-field vectors all along both sides of each ribbon. We arrange both ribbons such that they touch at one point and the B vectors are antiparallel there. This is required for the reconnection of B field lines. Next we staple the ribbons together to the left and right of the contact point and cut the ribbons in between the two staples, i.e., perform the actual "reconnection." When we are finished, there will be little flaps of paper next to the staple; ignore them or fold them over.

What we have obtained is one loop that has two complete (360°) twists as shown in Fig. 9(c). Since both twists are right handed, each twist contributes an amount of Φ^2 to the total helicity. Thus the helicity of the reconnected flux tubes is still $2\Phi^2$, the same helicity that we started with. Therefore, we have demonstrated that helicity is indeed preserved during reconnection.

By the way, as we have seen in one of our previous exercises, we can easily change the two 360° twists into the configuration displayed in Fig. 9(d). Measuring the two crossings with our *pencil helicity meter* we also obtain a total helicity of $2\Phi^2$.

VII. CONCLUSION

Although the systems in nature in which helicity occurs may be quite complex in and of themselves, the concept of helicity is easy to understand and may be demonstrated with the simplest of equipment.

ACKNOWLEDGMENT

The authors express their gratitude to Richard Cohen and to Jackie Payne for their diligence in preparing the figures for this article.

APPENDIX

The flux Φ of the magnetic field \mathbf{B} across a surface S can be expressed either in terms of the magnetic field \mathbf{B} or its associated magnetic vector potential \mathbf{A} ($\mathbf{B} = \nabla \times \mathbf{A}$) as

$$\Phi = \int_S \mathbf{B} \cdot d\mathbf{S} = \int_S (\nabla \times \mathbf{A}) \cdot d\mathbf{S} = \oint_C \mathbf{A} \cdot d\mathbf{x}, \quad (\text{A1})$$

where $d\mathbf{S} = \hat{\mathbf{n}} dS$ denotes a vector normal to the area element dS and C is a closed curve bounding the area S . The line integration is done in a right-handed sense. The total helicity of n arbitrarily interlinked, knotted, and twisted flux tubes is obtained by integrating Eq. (2) over all volumes V_i of these flux tubes. For the i th flux tube we have

$$H_i = \int_{V_i} \mathbf{A} \cdot \mathbf{B} d^3x \quad (i = 1, 2, \dots, n). \quad (\text{A2})$$

If we now apply this formula to calculate the total helicity of two singly linked flux tubes (Fig. 3) we obtain for the first volume

$$H_1 = \int_{V_1} \mathbf{A} \cdot \mathbf{B} d^3x = \oint_{C_1} \mathbf{A} \cdot \Phi_1 d\mathbf{x} \quad (\text{A3})$$

upon performing the integration across the cross section of the first flux tube. Since Φ_1 is constant along flux tube one, we can take it outside of the integral and we see that the integration along C_1 simply picks up the flux Φ_2 , i.e.,

$$H_1 = \Phi_1 \oint_{C_1} \mathbf{A} \cdot d\mathbf{x} = \Phi_1 \Phi_2. \quad (\text{A4})$$

Similarly, we obtain for the second volume

$$H_2 = \int_{V_2} \mathbf{A} \cdot \mathbf{B} d^3x = \Phi_2 \oint_{C_2} \mathbf{A} \cdot d\mathbf{x} = \Phi_2 \Phi_1 \quad (\text{A5})$$

and so the total helicity amounts to

$$H_{\text{tot}} = H_1 + H_2 = 2\Phi_1 \Phi_2. \quad (\text{A6})$$

¹ N. A. Salingaros, "On solutions of the equation $\nabla \times \mathbf{a} = k\mathbf{a}$," *J. Phys. A: Math. Gen.* **19**, L101–L104 (1986).

² N. A. Salingaros, "On solutions of the equation $\nabla \times \mathbf{a} = k\mathbf{a}$: II. The magnetic force-free model," *J. Phys. A: Math. Gen.* **19**, L705–L708 (1986).

³ N. A. Salingaros, "Magnetic force-free configurations for thermonuclear fusion," *Phys. Essays* **1**, 92–101 (1988).

⁴ E. R. Priest, "Introduction," in *Solar Flare Magnetohydrodynamics*, edited by E. R. Priest (Gordon and Breach, New York, 1981), pp. 1–46.

⁵ J. Birn and K. Schindler, "Two-ribbon flares: Magnetostatic equilibria," in *Solar Flare Magnetohydrodynamics*, edited by E. R. Priest (Gordon and Breach, New York, 1981), pp. 337–378.

⁶ G. W. Pneuman, "Two-ribbon flares: (Post)-flare loops," in *Solar Flare Magnetohydrodynamics*, edited by E. R. Priest (Gordon and Breach, New York, 1981), pp. 339–428.

⁷ R. Lüst and A. Schlüter, "Kraftfreie Magnetfelder," *Z. Astrophys.* **34**, 263–282 (1954).

⁸ Y. Nakagawa, M. A. Raadu, D. E. Billings, and D. McNamara, "On the topology of filaments and chromospheric fibrils near sunspots," *Solar Phys.* **19**, 72–85 (1971).

⁹ Y. Nakagawa and M. A. Raadu, "On practical representation of magnetic field," *Solar Phys.* **25**, 127 (1972).

¹⁰ C. W. Barnes and P. A. Sturrock, "Force-free magnetic field structures and their role in solar activity," *Astrophys. J.* **174**, 659–670 (1972).

¹¹ R. P. Lepping, J. A. Jones, and L. F. Burlaga, "Magnetic field structure of interplanetary magnetic clouds at 1 AU," *J. Geophys. Res. A* **95**, 11957–11965 (1990).

¹² D. R. Wells, "Axially symmetric force-free plasmoids," *Phys. Fluids* **7**, 826–832 (1964).

¹³ J. B. Taylor, "Relaxation and magnetic reconnection in plasmas," *Rev. Mod. Phys.* **58**, 741–763 (1986).

¹⁴ A. Janos, G. W. Hart, C. H. Nam, and M. Yamada, "Global magnetic fluctuations in Spheromak plasmas and relaxation toward a minimum-energy state," *Phys. Fluids* **28**, 3667–3675 (1985).

¹⁵ L. Woltjer, "A theorem on force-free magnetic fields," *Proc. Natl. Acad. Sci.* **44**, 489–491 (1958).

¹⁶ In 1987, Salingaros pointed out, by showing that the 2nd derivative is equal to zero rather than larger than zero, that these presumed minimum energy states are metastable saddle point configurations (cf. Ref. 17).

¹⁷ J. B. Taylor, "Relaxation of toroidal plasmas and generation of reverse magnetic fields," *Phys. Rev. Lett.* **33**, 1139–1141 (1974).

¹⁸ N. A. Salingaros, "An alternative description of the reversed-field toroidal plasma pinch, and prediction of the critical pinch parameter," *Hadronic J.* **10**, 109–116 (1987).

¹⁹ E. P. Butt, A. A. Newton, and A. J. L. Verhage, "Experimental observation of the self reversal of toroidal magnetic field in pinches," in *Pulsed High Beta Plasmas*, edited by D. E. Evans (Pergamon, Oxford, 1976), pp. 419–423.

²⁰ C. A. Norman and J. Heyvaerts, "The final state of a solar flare," *Astron. Astrophys.* **124**, L1–L3 (1983).

²¹ M. A. Berger, "Rigorous new limits on magnetic helicity dissipation in the solar corona," *Geophys. Astrophys. Fluid Dyn.* **30**, 79–104 (1984).

²² A. Königl and A. R. Choudhuri, "Force-free equilibria of magnetized jets," *Astrophys. J.* **289**, 173–187 (1985).

²³ B. B. Kadomtsev, "Tokamak plasma self-organization," *Comments Plasma Phys. Controlled Fusion* **11**, 153–163 (1987).

²⁴ A. Janos, "Magnetic flux conversion and relaxation toward a minimum-energy state in spheromak plasmas," *Phys. Fluids* **29**, 3342–3355 (1986).

²⁵ B. U. Ö. Sonnerup, "Magnetic field reconnection," in *Solar System Plasma Physics. Vol. III*, edited by L. J. Lanzerotti, C. F. Kennel, and E. N. Parker (North-Holland, Amsterdam, 1979), pp. 47–108.

²⁶ V. M. Vasyliunas, "Theoretical models of magnetic field line merging I," *Rev. Geophys. Space Phys.* **13**, 303–336 (1975).

²⁷ R. L. Stenzel, W. Gekelman, and J. M. Urrutia, "Lessons from laboratory experiments on reconnection," in *Solar Wind Interactions*, edited by C. T. Russell, *Adv. Space Res.* **6**, 135–147 (1986).

²⁸ L. C. Lee, Z. F. Fu, and S.-I. Akasofu, "Multiple X-line reconnection in the Earth's magnetosphere," in *Magnetotail Physics*, edited by A. T. Y. Lui, (Johns Hopkins U.P., Baltimore, 1987), pp. 191–197 (and references therein).

²⁹ N. F. Ness, "Magnetotail research: The early years," in *Magnetotail Physics*, edited by A. T. Y. Lui (Johns Hopkins U.P., Baltimore, 1987), pp. 11–20 (and references therein).

³⁰ L. A. Frank, "Plasmas in the Earth's magnetotail," *Space Sci. Rev.* **42**, 211–240 (1985).

³¹ L. Neuwirth, "The theory of knots," *Sci. Am.* **240**(6), 110–124 (1979).

³² C. T. Russell and R. C. Elphic, "Observation of magnetic flux ropes in the Venus ionosphere," *Nature* **279**, 616–618 (1979).

³³ H. K. Moffatt, *Magnetic Field Generation in Electrically Conducting Fluids* (Cambridge U.P. Cambridge, 1978), pp. 14–17.

³⁴ This demonstration is suitable as a class demonstration. It will give an enlightening answer to the question: "Can there be helicity if there are no linkages and no knots?" It will prevent the students from making the following erroneous conclusion: "The absence of knots and links implies no helicity!" Since the single twist in the electric cable is most likely not visible even in the first row, the students simply see one O-type configuration with no links and no knots, and thus they will most likely assume that this configuration has no helicity. But much to their surprise, this particular O-type configuration is a configuration containing helicity.

³⁵ The extension to the case of arbitrarily linked and knotted topological configurations consisting of several flux tubes with different fluxes is straightforward. For example, a flux tube with flux Φ_i crossing over a flux tube with flux Φ_j would contribute an amount of plus or minus $\Phi_i \Phi_j$ to the total helicity of that configuration. The sign, "+" or "–" can be determined in the same way as for flux tubes containing the same flux Φ , using the famous *pencil helicity meter*.

³⁶ M. A. Berger and G. B. Field, "The topological properties of magnetic helicity," *J. Fluid. Mech.* **147**, 133–148 (1984).

³⁷ Patent not pending!